UNDULATOR RADIATION DOSE CAUSED BY SYNCHROTRON RADIATION AT THE EUROPEAN XFEL

S. Liu[†], DESY, Hamburg, Germany
Y. Li, F. Wolff-Fabris, XFEL.EU, Schenefeld, Germany

Abstract

Radiation damage of the undulators is a big concern for the light sources. At the European XFEL (EuXFEL), dosimeters based on on-line Radfets are used for the undulator radiation dose measurements. However, since the Radfets are not only sensitive to the electrons and neutrons but also to the photons, it can capture the synchrotron radiation (SR) generated in the undulators, which is not considered to be the main source for undulator radiation damage. Therefore, it is important to estimate the contribution of synchrotron radiation to the radiation doses measured by the Radfets. For this purpose, we have first calculated the synchrotron radiation profile using SPECTRA, and then put the profile into the tracking code BDSIM to track it through the whole undulator beam line. The radiation doses from SR have been simulated and compared with the measured values. The differences in the radiation doses measured by the Radfets before and after Pb shielding will also be presented.

INTRODUCTION

The European XFEL (EuXFEL) has started user operation since Sept. 2017 [1-4]. It operates in pulse mode with a maximum repetition rate of 4.5 MHz (27000 bunches/s). The maximum beam power that can be generated is more than 500 kW. The high repetition rate and high power posse big concern for the radiation damage of the undulators. To monitor the radiation damage of the undulators, diagnostic undulators (DU) are installed at the very beginning of the three undulator systems (SASE1, SASE2 and SASE3). For the radiation measurements, dosimeters based on on-line Radfets are installed at each undulator segment [5].

It was previously reported that relative high undulator doses have been measured especially in the DU [6]. However, previous studies have also shown that the high radiation dose and demagnetization of the DU is mainly due to miss-steered beam hitting the vacuum chamber transition. And the doses measured at the downstream undulators were supposed to be due to the spontaneous synchrotron radiation (SR) [7].

In this paper, we estimate the contribution of SR to the undulator radiation doses. First, the synchrotron radiation profile is calculated using SPECTRA [8], and then the profile is loaded into the tracking code BDSIM [9] to track it through the undulators, from which the radiation doses in the undulators have been recorded and compared with the recently measured values. Finally, the differences in the radiation doses measured by the Radfets before and after Pb shielding are presented.

---

† shan.liu@desy.de

SYNCHROTRON RADIATION CALCULATIONS

The spontaneous radiation generated in the undulators has much larger divergence than the SASE. In the undulator system which is longer than 200 meters the SR beam may expand wide enough to reach the vacuum chamber. The powerful SR may interact with the vacuum chamber and generate secondary radiation contribution to the undulator dose.

The doses from the SR are expected to be less harmful than that from the electron beams. Nevertheless, it is necessary to evaluate the SR contribution to the doses. In order to do so, we simulated the phase space of the undulator spontaneous radiation using SPECTRA. The parameters used in the simulations are from the European XFEL SASE1 beam line, which are listed in Table 1.

Table 1: Parameters for the SR Simulations

Beam energy	14 GeV
Average current	1×10^{-10} A
Bunch charge	100 pC
Peak current	4 kA
Natural Emittance	2.336×10^{-11} mrad
Undulator period	40 mm
Undulator length	5 m
Undulator parameter K	2.70304
1st harmonic photon energy	10 keV

First we simulated the total flux spectrum with respect to the photon energy. Fig. 1 shows the simulation results. It can be seen that the flux continuously drops until the 20th harmonics. Therefore we simulated the flux density in the phase space (x,x',y,y') at each harmonic below the 20th harmonics.
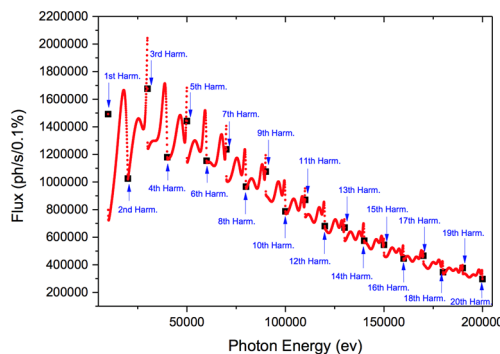

Figure 1: The spectrum of the total SR flux with respect to the photon energy.

In the far field approximation the transverse beam size expands linearly with respect to the observer's distance.

Therefore the photon transverse position equals the product of its divergence angle and the distance: $x=x'\cdot d$ and $y=y'\cdot d$, where d denotes to the observer's distance. In our simulation 0.08 mrad is chosen as observation angle, and 50 m is chosen as observation distance.

In Fig. 2 the simulated flux density distributions in the phase space (x', y') are plotted. The left plot shows the results of the 1st harmonic and the right plot shows the 2nd harmonic. Such flux density phase space is simulated for each SR harmonic up to the 20th. Loading the results to the tracking code BDSIM, which takes into account the vacuum chamber geometries, the radiation dose by SR is further calculated.
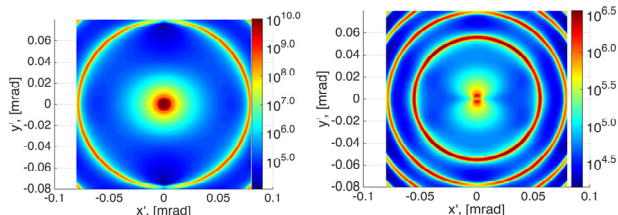

Figure 2: The flux density distribution in the phase space (x',y') of the 1st harmonic (left) and the 2nd harmonic (right).

BDSIM TRACKING SIMULATIONS

Figure 3 shows the layout of the geometry used in the BDSIM simulation. It includes undulator cells, constitutes by magnets and poles and a vacuum chamber with elliptical hole (see Fig. 3 right plot), an absorber and a quadrupole between the cells. The undulator chamber material is Al and the other chambers in the intersection are made of stainless steel.
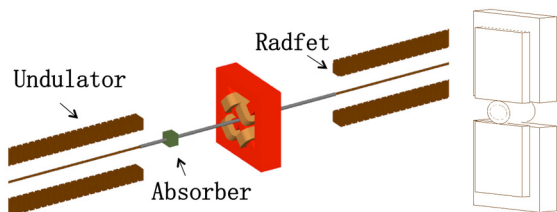

Figure 3: Geometry used in the BDSIM simulation: undulator cells with transition section (left) and zoomed geometry of the undulator magnet and pole together with vacuum chamber (right).

The drawing of the absorber and the simplified sketch used in BDSIM are shown in Fig. 4. Since the absorber is designed for SR absorption, its geometry is quite important in the simulation. In the simulation, we found out that the thickness and the apertures of the absorber significantly affect the radiation doses from the SR. Therefore, we presented the apertures in more detail by combining four layers of Copper block with different apertures. The first two layers (6 mm and 9 mm thick) are with the same aperture as the undulator vacuum chamber (2a=15 mm, 2b=8.8 mm ellipse), followed by the absorber layer (3 mm thick with an ellipse aperture of 2a=9 mm, 2b=8 mm), and one more layer (22.2 mm thick) with the same aperture as the Quadrupole (ø 10 mm).
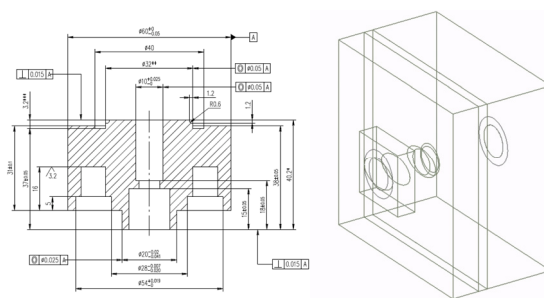

Figure 4: Drawing of the absorber (left) and the simplified sketch (right) used in BDSIM simulation.

The simulation starts at the observation point (~50 m) and the same SR distribution is added after each undulator section (6.1 m long). The photon number for different photon energy is applied as "weight" factor and the G4EmStandardPhysics list is used in the simulation. The energy losses (in GeV) in each element are recorded and normalized to the dose (in Gy/C) for the input electron beam charge of 100 pC. The undulator magnets and poles are put into BDSIM together with the vacuum chamber as a single element (constrained by the BDSIM geometry input form, see Fig.3 right plot). Therefore, two simulations have been performed with and w/o magnets and poles (with the same seed number) and the dose absorbed by the vacuum chamber is subtracted afterwards to get the real dose on the undulator. In the simulation, we found out that most SR is absorbed by the absorber (mainly by the absorber layer), however, there is still some residual part (mainly higher harmonics) of the SR which reaches the undulator. The simulated radiation doses along the undulators are shown in Fig. 5. The red curve represents the doses recorded by the 1st magnet and pole of each undulator, near the position where the Radfets are installed, while the blue curve shows the averaged dose over each 5 m long undulator segment.
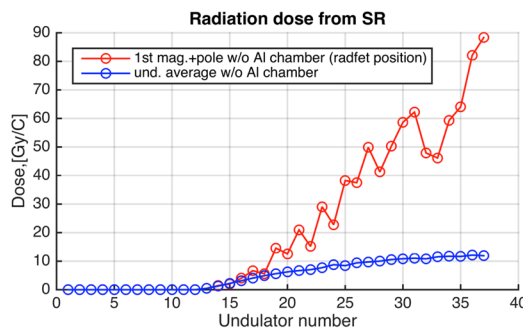

Figure 5: Radiation dose from SR recorded by the 1st magnet and pole of each undulator (red), and by the undulator segment in average (blue). The dose contribution from the Al vacuum chamber is subtracted in both curves.

From Fig. 5, one can see that at the 1st magnet and pole positions, the doses are higher than the averaged values, due to the radiation shower generated in the transition section, which has much larger opening angles and fluctuates from shot to shot. This also explains the fluctuation in the

red curve, which is mainly caused by the statistic fluctuations. Since the Radfet dimension is much smaller than the magnet and pole, we would expect that it captures much less radiation showers. In this case the SR dose should be closer to the averaged doses over one undulator segment (blue curve).

COMPARISON WITH MEASUREMENTS

For the radiation measurements, two Radfets (upper and lower) are installed in front of each undulator and they move together with the undulator gap [5, 6].

Since 2017, the Radfets readout values are integrated and normalized to the total charge each week. The 12 weeks with lowest and highest dose per charge rate (from 2017 to summer 2018) are presented as cloud areas in Fig. 6 in green and in red, respectively. It is important to mention that the weeks with highest dose rates are mostly the machine study weeks with miss-steering events resulting in beam losses and the weeks with lowest rates are mostly the user run weeks. Besides, it is obvious that the first segments have much higher doses than the others. This is expected, since when the miss-steering events happen, they act as shielding for the downstream segments.

In Fig. 6 one can see that the average dose of the green weeks is around 10 Gy/C, which is quite consistent with the simulated averaged dose in the undulator (blue circle). However, in the simulation, no SR doses are accumulated before cell 13. This indicates that the losses observed before cell 13 may be caused by other sources (e.g. miss-steered beam during machine set-up).
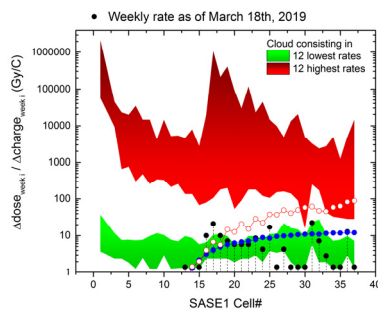

Figure 6: Weekly dose rate in SASE1 with the cloud consisting the 12 lowest (green) and highest (red) dose rates (from 2017 to summer 2018). The black dots represent the 12th week (March 18th) of 2019. For comparison, the results from simulation are also plotted in blue and red circles as in Fig. 5.

One example of dose rate during the user run week (12th week in 2019) is shown as black dots in Fig. 6. It can be seen that the measurable radiation dose starts at cell 13 and increases at cell 16. This confirms that, during stable user operation, the doses recorded by the Radfets after cell 13 are mostly due to SR. Meanwhile, it is worth to mention that, during this week of user run, only the first 25 undulators were used for lasing. The undulator gaps for the other cells were open. This explains the decrease of dose start from cell 26. However, another two dose peaks appeared at cell 31 and cell 36, the reason for these peaks is not known

yet. It may be caused by increased beam-gas scattering due to degraded vacuum level and increased beam halo extension.

In order to distinguish the source of different dose contributions, 4 mm thick Pb plates are added in front of the lower Radfets to shield the SR. Figure 7 shows the radiation doses accumulated from May 2017 to Jan. 2019 by the upper and lower Radfets for cell 3 and cell 31. It can be seen that almost no difference in dose between the upper and the lower Radfets can be observed at cell 3 before and after adding the shield. However, for cell 31, after adding the shield, the lower Radfets readout stays almost constant while the unshielded upper Radfets continues to accumulate doses. By comparing these two cells, we can see that the 4mm Pb shield makes difference for the downstream undulators and has almost no influence on the upstream ones. Therefore, we can conclude that the doses at the upstream undulators are mostly due to high energy electrons while the downstream ones are mostly dominated by low energy SR.
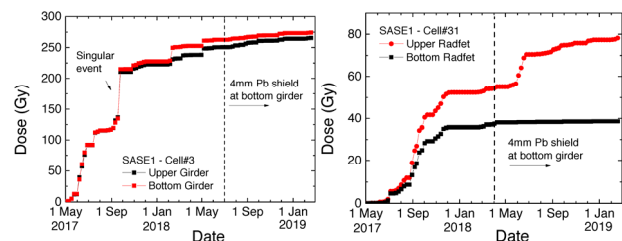

Figure 7: Radiation dose accumulated on upper (black) and bottom (red) Radfets in SASE1 undulator cell 3 and cell 31 from May 2017 to Jan. 2019. The dashed lines indicate the time when the bottom Radfets are shielded by the 4 mm Pb plates.

CONCLUSIONS AND FUTURE PLANS

We have performed SR tracking simulations in BDSIM using the SR profiles obtained from SPECTRA. From the simulation we calculated the possible radiation doses generated by the SR along the undulators. An averaged dose of around 10 Gy/C is obtained, which is in good agreement with the measurement data from the stable user run weeks. By comparing the simulation results with the measurements, we concluded that the doses measured at the upstream undulators are dominated by high energy electron beam losses while the downstream undulators suffers mainly from the low energy SR. This conclusion is further proved by the shielding of the Radfets.

In the future, tune-up beam stops are planned to be installed in front of the undulator beam lines, which will help to protect the upstream undulators from miss-steered beam. Meanwhile, all the Radfets will be shielded by Pb plates to filter the dose from SR.

ACKNOWLEDGEMENTS

MC2: Photon Sources and Electron Accelerators

T15 Undulators and Wigglers

REFERENCES

[1] M. Altarelli, R. Brinkmann *et al.*, "XFEL: The European X-Ray Free-Electron Laser Technical Design Report", DESY, Hamburg, Germany, DESY 2006-097, 2006.

[2] H. Weise and W. Decking, "Commissioning and First Lasing of the European XFEL", in *Proc. 38th Int. Free Electron Laser Conf. (FEL'17)*, Santa Fe, NM, USA, Aug. 2017, pp. 9-13. doi:10.18429/JACoW-FEL2017-MOC03

[3] M. Scholz, "FEL Performance Achieved at European XFEL", in *Proc. 9th Int. Particle Accelerator Conf. (IPAC'18)*, Vancouver, Canada, Apr.-May 2018, pp. 29-33. doi:10.18429/JACoW-IPAC2018-MOZGBD2.

[4] W. Decking *et al.*, "Status of the European XFEL", presented at the 10th Int. Particle Accelerator Conf. (IPAC'19), Melbourne, Australia, May 2019, paper TUPRB020, this conference.

[5] F. Schmidt-Foehre, L. Froehlich, D. Noelle, R. Susen, and K. Wittenburg, "Commissioning of the New Online-Radiation-Monitoring-System at the New European XFEL Injector with First Tests of the High-Sensitivity-Mode for Intra-Tunnel Rack Surveillance", in *Proc. 4th Int. Beam Instrumentation Conf. (IBIC'15)*, Melbourne, Australia, Sep. 2015, pp. 585-589. doi:10.18429/JACoW-IBIC2015-WECLA02.

[6] F. Wolff-Fabris, J Pflueger, F. Schmidt-Föhre and F. Hellberg, "Status of radiation damage on the European XFEL undulator systems". 2018 *J. Phys.: Conf. Ser.* vol. 1067 p. 032025.

[7] S. Liu, W. Decking, and F. Wolff-Fabris, "Study of Possible Beam Losses After Post-Linac Collimation at European XFEL", in *Proc. 9th Int. Particle Accelerator Conf. (IPAC'18)*, Vancouver, Canada, Apr.-May 2018, pp. 4092-4095. doi:10.18429/JACoW-IPAC2018-THPMF022.

[8] T. Tanaka and H. Kitamura, "SPECTRA: a synchrotron radiation calculation code", *Journal of synchrotron radiation,* vol. 8(6), pp. 1221-1228, 2001.

[9] I. Agapov, G.A. Blair, S. Malton and L. Deacon, "BDSIM: A particle tracking code for accelerator beam-line simulations including particle–matter interactions" *Nucl. Instr. Meth. A*, vol. 606(3), pp. 708-712, 2009.